

# Critical Issues in Short-cut Modelling of Massive Carbon Dioxide Releases

Emilio Palazzi, Fabio Currò, Tomaso Vairo, Bruno Fabiano\*

DICCA – Civil, Chemical and Environmental Engineering Department - University of Genoa, Via Opera Pia, 15 – 16145 Genoa, Italy  
[brown@unige.it](mailto:brown@unige.it)

In case of accidental gaseous releases, the detailed analysis of rather complicated situations (partial confinement, irregular shapes, unsteady-state) usually requires the use of sophisticated integral models and/or CFD calculations, but when conservative results are enough, especially in preliminary hazard assessment, analytical models can be conveniently applied. This paper presents a very simple analytical model accounting also for wind effect on accidental release evolution, suitable to be adopted as short-cut evaluation tool in case of accidental carbon dioxide semi-continuous release at high speed (jet), and nearly instantaneous releases from high-pressure systems. It may allow a preliminary evaluation of emergency actions, in case of a massive and deadly release of carbon dioxide from a storage site, or due to natural event, once properly defined the source term and refined for possible thermal effects.

## 1. Introduction

CCS is a key reduction strategy to limit CO<sub>2</sub> emissions, but its development is strongly limited mostly by high costs, social and political acceptability, thus requiring to carry out an exhaustive perspective plan to cover all uncertainties linked to it (Viebahn et al., 2015). Examples include the storage scenarios and the need of an appropriate analysis of the site and consequence modelling, to prevent or mitigate possible leakages (Hansson & Bryngelsson, 2009). The development of a simplified bow-tie approach for CO<sub>2</sub> storage may rely on 11 main hazardous events (Le Guéan et al., 2011), i.e.:

- Leakage via an operational well
- Mechanical disruption nearby the injection well
- Mechanical disruption at the storage complex scale
- Expected lateral extent exceeded
- Leakage due to sealing deficiency of the caprock
- Leakage via existing faults
- Leakage via an abandoned well
- Accumulation in a secondary reservoir
- Flow modifications
- Disruption by a later activity
- Disruption by a natural earthquake.

However, these methods often require precise probability values to support the evaluation and, in practical applications, there are often many knowledge limitations. As stated by Vairo et al., (2021), due to incomplete statistics and knowledge, there will be some uncertainties on the likelihood and interdependence of root risk events in Fault Tree (FT) and events in Event Tree (ET), which may lead to unrealistic results. Generally speaking, the consequences of CO<sub>2</sub> leaks can be divided into two groups: global and local. The global ones are connected with leakage into the atmosphere, not considering space and time so reducing the effectiveness of geological storage and leading to an increase in CO<sub>2</sub> concentration into the atmosphere. Local consequences can be short or long term and can fall into three categories, namely (i) health and safety, (ii) environmental and (iii) equity. For the first two, there are natural and anthropogenic analogues (such as incidents in NG pipelines),

which may help in developing risk assessment related to CO<sub>2</sub> geological storage. Mazzoldi et al. (2013) evidenced by simulation runs a peculiar feature of CO<sub>2</sub> plumes and consequent affected from ruptured high-pressure pipelines: more than 25% of the CO<sub>2</sub> contour at 1 m above the ground is composed of a rather flat tongue approximately 20 m wide and extending nearly 100 m from the break. A step forward was proposed by Li et al. (2014), who performed experimental runs on leakage from a supercritical CO<sub>2</sub> pipeline, observing the multiphase jet and the formation of a dry ice bank outside of the nozzle. The leakage flow, after a brief transient state, reaches a steady value, while the amount of carbon dioxide, still inside the pipeline keeps decreasing.

**2. Instantaneous release short-cut evaluation**

In developing a short-cut approach, we started from the consideration by Chow et al. (2009) for an instantaneous release scenario under 22 different combinations of wind, topography, atmospheric stability and release strength, summarized as follows:

- In wind absence, CO<sub>2</sub> spreads laterally over flat terrain and a concentrated CO<sub>2</sub> plume tends to hug the ground, migrating towards the sites with the lowest elevations.
- Owing to density effects, CO<sub>2</sub> spreads more quickly than a neutrally-buoyant gas so that (although counter-intuitive) it resulted that ground level concentrations can drop in a shorter time for a dense gas under calm conditions.
- CO<sub>2</sub> acts as a dense gas under no, or weak wind conditions, but in wind presence from 2 m·s<sup>-1</sup>, the behavior is affected by transport and diffusion phenomena sweeping away the plume.

As a result, in some circumstances, with stable atmospheric conditions and low wind velocities, CO<sub>2</sub> might pond in a populated topographic low near a large CO<sub>2</sub> release from a pipeline or a storage site and be lethal at a distance considerably larger than the danger zone for natural gas explosions. However, there is no accord to the safety distance even from a pipeline of natural gas or carbon dioxide, while the definition of the critical dose  $D_c$  requires a proper refinement, as detailed in Palazzi et al., 2016a and CO<sub>2</sub> toxicity threshold summarized in Table 1. The critical concentration  $y_c$  may be used to identify, by means of an appropriate model of atmospheric dispersion, the distance from the release  $r_c$ , beyond which  $y < y_c$  and the unwanted event could not theoretically happen. On the other hand, this effect can rise just if the duration of the exposition at the concentration  $y_c$  is not lower than the critical value  $\tau_c$ .

The evolution in time of an instantaneous release under no wind conditions, is schematically depicted in Figure 1; after a rapid initial dilution, which is necessary to complete the sublimation (S→V) of the CO<sub>2</sub>, the amount of motion runs out, because of the greater density respect to the air and because of the friction with the ground. A dense cloud is formed, subject to shedding by gravity; it dilutes with the air while radially propagates itself. Because the mechanism of formation of the cloud is different if compared to the one relative to the semicontinuous vertical jet, it is necessary to modify the hypothesis concerning the characteristics of the cloud after the initial phase of dispersion, even to take into account the fact that, under certain situations here treated, the above-mentioned hypotheses would be too precautionary.

Table 1: Carbon dioxide levels of toxicity.

Concentration $y_c$	Exposure Time $\tau_c$ [s]	Effects	Source	Dose $D_c$ [s]
0.25	60	Death	(Mazzoldi et al, 2013)	15
0.10	600 <sup>(1)</sup>	Death	(Mazzoldi et al, 2013)	60
0.04	1,800	IDLH	NIOSH	72

(1) Precautionary assumption, in the given range: 600 – 750 (Mazzoldi et al., 2013)

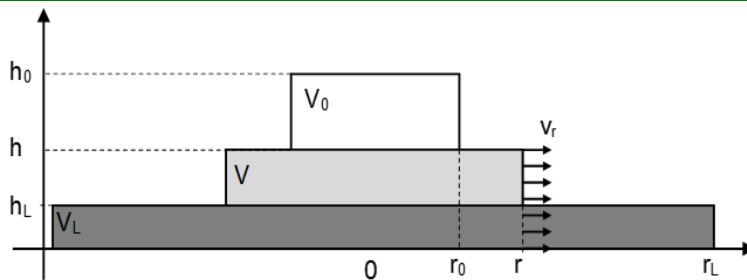


Figure 1: Simplified time evolution of an instantaneous release, from  $V_0$  to  $V_L$ .

Table 2: Transition point from jet phase to cloud diffusion under the hypothesis of Van Ulden, for different values of wind velocity.

$u$ [m·s <sup>-1</sup> ]	$u^*$ [m·s <sup>-1</sup> ]	$v_r$ [m·s <sup>-1</sup> ]	$m_{rL}$ [kg]	$r^* = \beta_i \cdot m_r^{1/2} \cdot v_r^{*-1}$ [m]	$r_r$ [m]
2	0.132	0.264	$9.5 \cdot 10^5$	$4.3 \cdot 10^3$	$1.7 \cdot 10^3$
			$1.8 \cdot 10^9$	$1.9 \cdot 10^6$	$6.4 \cdot 10^4$
10	0.66	1.32	$4.8 \cdot 10^7$	$6.3 \cdot 10^3$	$3.3 \cdot 10^3$
			$6.6 \cdot 10^{10}$	$2.3 \cdot 10^5$	$9.6 \cdot 10^4$
20	1.32	2.64	$3.1 \cdot 10^8$	$8.0 \cdot 10^3$	$4.9 \cdot 10^3$
			$3.5 \cdot 10^{10}$	$2.7 \cdot 10^5$	$1.3 \cdot 10^5$

The simplified approach here discussed relies on previous simulation results validated by Palazzi et al, (2016a, 2016b) obtained under no wind conditions, as follows:

$$v_r = \frac{1}{r} \sqrt{\frac{\rho_0 - \rho_a}{\rho_a} \frac{g}{\pi \rho_0 W_0} m_r} \quad (1)$$

$$r^2 = r_0^2 + 2\beta_i m_r^{1/2} t \cong 2\beta_i m_r^{1/2} t \quad (2)$$

$$\beta_i = \frac{(\rho_0 - \rho_a) g}{\rho_a \rho_0 \pi W_0} \quad (3)$$

Following the reasoning of van Ulden (1974) the transition from the jet phase to cloud corresponds to the attainment of the condition  $v_r = 2u^*$ , i.e., from Eq. (1):

$$v_r = \frac{\beta_i}{r} (m_r)^{1/2} \quad (4)$$

As shown in Table 2, under the following conditions:  $T = 273$  K,  $P = 10$  MPa,  $r_0 = 0$ ,  $\beta_i = 1.20$ , the transition point is never attained, being  $r < r^*$  and  $v_r \neq 2 \cdot u^*$ .

In case of dispersion under no wind conditions, the relevant contribution to turbulent diffusion is due to the term  $v_r$ , while in case of moderate windy conditions it is assumed that after the jet phase transition, the relevant cloud dilution effect is connected to the wind velocity  $u$ . Under the simplifying assumptions of flat terrain, no obstructions, no local concentration fluctuation, no chemical reaction, the unsteady – state behavior of a nearly-instantaneous carbon dioxide release, near the ground, can be described by Eq(5).

$$\frac{dV}{dt} = k\pi r^2 u \quad (5)$$

From Eq (2), one can write:

$$dt = \frac{r}{\beta_i m_r^{1/2}} dr \quad (6)$$

and

$$dV = \frac{k\pi u}{\beta_i m_r^{1/2}} r^3 dr \quad (7)$$

By integration, one can easily obtain:

$$V - V_0 = \frac{1}{4} \frac{k\pi u}{\beta_i m_r^{1/2}} (r^4 - r_0^4) \quad (8)$$

For the purposes of the dose calculation, it is fundamental to determine the variations in the carbon dioxide concentration,  $y(r)$ , during the dilution of the release. In a conservative way, the dose calculation is referred to the CO<sub>2</sub> concentration on the axis of the cloud  $y_a$  that is assumed according to van Ulden (1974) and original wind tunnel experimental runs at the laboratory scale on jet scenarios, corresponding to the double of the mean concentration. Being:

$$V - V_0 = \frac{m_r}{\rho_a} \left( \frac{1}{w} - \frac{1}{w_0} \right) \quad (9) \quad \frac{1}{w} - \frac{1}{w_0} = \frac{M_a}{M_r} \left( \frac{1}{y} - \frac{1}{y_0} \right) \quad (10)$$

Taking in account Eq(8) one can obtain:

$$y = y_0 [1 + \xi^2 (r^4 - r_0^4)]^{-1} \quad (11)$$

being by definition:

$$\xi^2 = \frac{1}{4} \frac{k\pi \rho_a y_0 u}{\beta_i m_r^{3/2}} \quad (12)$$

From Eq. (11), it is possible calculating the cloud radius as follows:

$$r = \left[ r_0^4 + \frac{1}{\xi^2} \left( \frac{1}{y} - \frac{1}{y_0} \right) \right]^{1/4} \quad (13)$$

On the basis of the previous simplifying assumptions, the dose can be calculated as:

$$D = \int_{t_1}^{t_2} y_a(t) dt = \int_{t_1}^{t_2} 2y(t) dt = \int_{r_1}^{r_2} 2y(r) \frac{r}{\beta m_r^{1/2}} dr \quad (14)$$

And taking into account Eq(5), it follows

$$D = \int_{r_1}^{r_2} 2y_0 [1 + \xi^2 (r^4 - r_0^4)]^{-1} \frac{r}{\beta m_r^{1/2}} dr \quad (15)$$

After straightforward algebraic manipulations, one can finally calculate:

$$D = \frac{y_0}{\beta_i m_r^{1/2} \xi \sqrt{1 - r_0^4 \xi^2}} \left[ \arctg \frac{\xi}{\sqrt{1 - r_0^4 \xi^2}} \left( \frac{2\beta m_r^{1/2}}{u} - r_1 \right)^2 - \arctg \frac{\xi}{\sqrt{1 - r_0^4 \xi^2}} r^2 \right] \quad (16)$$

where  $r=r(y)$  is easily calculated by means of Eq. (13).

The value of  $r_0$  is equal to 0, in the case of no wind condition (model a). In the case of wind presence, it can be calculated under the simplifying hypothesis that at the end of initial expansion phase, the cloud, can be approximated by an equivalent equilateral cylinder (model b).

$$r_0 = \left( \frac{1}{2\pi w_0 \rho_0} \right)^{1/3} m_r^{1/3} \quad (17)$$

Following a different simplified approach (model c),  $r_0$  is estimated by imposing that the initial expansion phase ends when dilution velocities along the down and transversal wind direction are equal, so that it follows:

$$r_0 = \left( \frac{2\beta_i}{\pi w_0 \rho_{0u}} \right)^{1/3} m_r^{3/8} \quad (18)$$

### 3. Results and discussion

We applied the framework making reference to the different working hypotheses previously outlined in Table 2 and adopting as illustrative examples 3 wind velocities, namely 2, 10, 20  $\text{m}\cdot\text{s}^{-1}$ , even if the case of high wind velocity may be of scarce practical interest. The explored operative conditions are summarized in Table 3, selected from operative range commonly adopted in storage and transport activities, derived from literature (Webber, 2011), as follows:  $10 \leq p_i \leq 20$  [MPa],  $273 \leq T_i \leq 323$  [K].

Table 3: Explored operative conditions.

	Run I	Run II	Run III	Run IV
$T_i$ [K]	273	273	323	323
$p_i$ [MPa]	10	20	10	20

In this regard, because of the high  $\Delta p$  value, the velocity of the fluid in the efflux section is quite high (100 to 250  $\text{m}\cdot\text{s}^{-1}$ ). The physico-chemical properties of  $\text{CO}_2$  and, in particular, the critical point ( $p_c=7.3825$  MPa;  $T_c=304.21$  K), and the sublimation point at atmospheric pressure ( $T_s=194.65$  K), imply the possible presence of three phases, although not simultaneously. Performed calculations provide only an estimate aiming at evaluating the sensitivity of attained results on the different possible calculations of initial cloud dimension,  $r_0$ .

Table 4: Comparison between values of critical released mass and critical distance (model a, b, c).

$u$ [ $\text{m}\cdot\text{s}^{-1}$ ]	$m_{rc}$ [kg]	Run II			$m_{rc}$ [kg]	Run III			$m_{rc}$ [kg]	Run IV		
		$r_c$ [m]	$r_c$ [m]	$r_c$ [m]		$r_c$ [m]	$r_c$ [m]	$r_c$ [m]		$r_c$ [m]		
		(a)	(b)	(c)		(a)	(b)	(c)		(a)	(b)	(c)
2	$1.2 \cdot 10^6$	895	892	876	$3.2 \cdot 10^6$	538	536	528	$9 \cdot 10^5$	851	848	834
2	$5.0 \cdot 10^9$	27,684	27,729	27,556	$4.1 \cdot 10^8$	8471	8466	8408	$5.0 \cdot 10^9$	17,043	17,033	16,930
10	$5.6 \cdot 10^7$	3351	3320	3231	$1.9 \cdot 10^7$	2319	2301	2253	$5.6 \cdot 10^7$	3393	3367	3392
20	$3.4 \cdot 10^8$	6439	6355	6170	$1.3 \cdot 10^8$	4705	4653	4553	$3.4 \cdot 10^8$	6683	6661	6453

It can be noticed that the maximum difference of the critical distance (defined as the maximum distance of release at which the exposition to CO<sub>2</sub> can provoke serious effects utilizing the refined dose approach) calculated under the three hypotheses is nearly 4%. The most conservative estimate corresponds to the simple and drastic approximation  $r_0 = 0$ , as schematically shown in Table 4.

Table 5: Comparison between critical distance  $r_c$  [m] obtained by jet release under no wind condition and the instantaneous massive release scenario.

	Jet scenario $u=0$	Instantaneous release $u = 10 \text{ m}\cdot\text{s}^{-1}$	Instantaneous release $u=20 \text{ m}\cdot\text{s}^{-1}$
Run I	6268	3361	6459
Run II	5900	3351	6479
Run III	2394	2319	4705
Run IV	3873	3393	6683

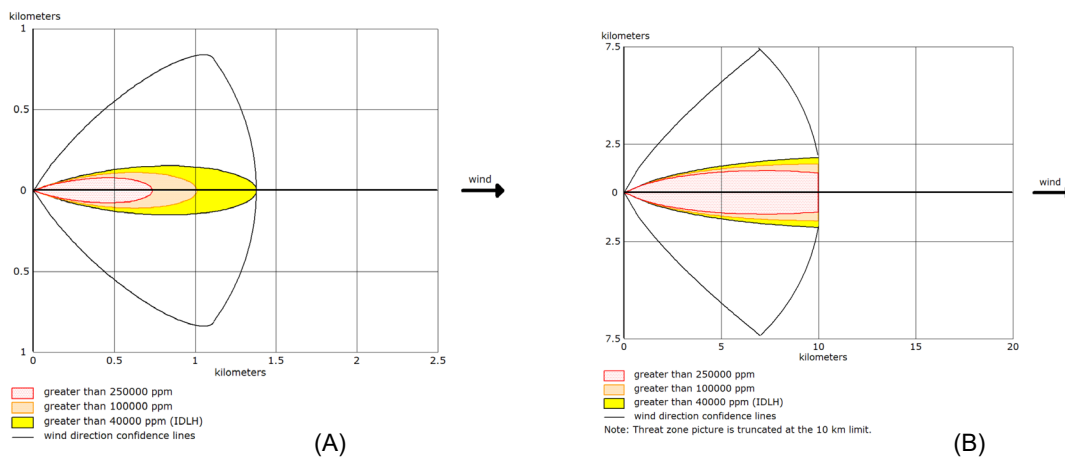


Figure 2: Footprints of the Aloha simulations A and B.

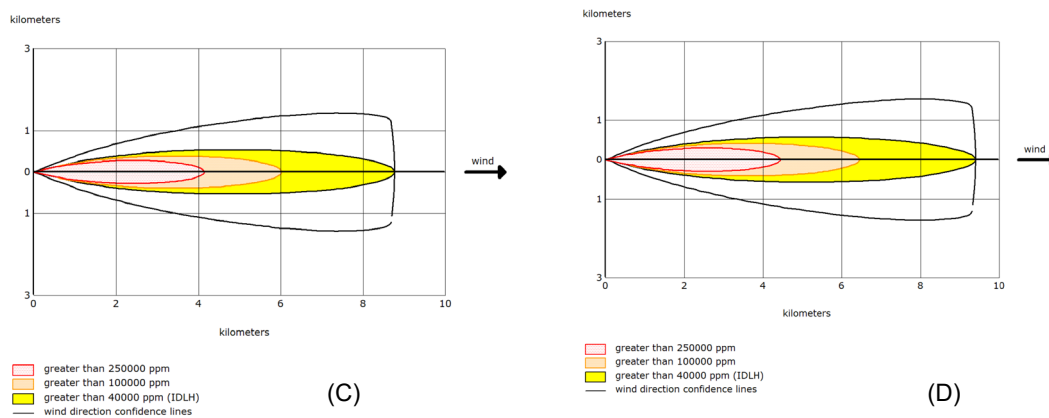


Figure 3: Footprints of the Aloha simulations C and D.

Table 5 allows an immediate comparison between the most conservative results obtained by a jet release under no wind condition (Palazzi 2016a) and the instantaneous massive release scenario.

Table 6: Aloha simulations conditions adopting as reference different CO<sub>2</sub> threshold values.

	Instantaneous release $m_{rc}$ [kg]	Wind speed $u$ [ $\text{m}\cdot\text{s}^{-1}$ ]	Temperature $T_i$ [K]	Pressure $p_i$ [MPa]
Run A	$1.2 \cdot 10^6$	2	273	20
Run B	$5 \cdot 10^9$	2	273	20
Run C	$5.6 \cdot 10^7$	10	273	20
Run D	$5.6 \cdot 10^7$	10	323	20

At last, we explored some situations by means of Aloha integral model, which is developed to plan emergency response in case of an actual accident and is therefore rather conservative. The set-up of Aloha is for general purpose and it is considered as a short-cut tool; we used it as a preliminary comparison to roughly highlight the model capabilities and degree of conservatism. Simulation conditions are summarized in Table 6, while the results of different runs are shown in Figures 2 and 3 with calculated threshold distances presented in Table 7.

Table 7: Threshold distances calculated with Aloha model adopting as different CO<sub>2</sub> reference values.

Aloha run	0.04 (mol/mol) IDLH	0.10 (mol/mol)	0.25 (mol/mol)
A	1.4 km	1 km	0.7 km
B	14.8 km	12.3 km	11.1 km
C	8.6 km	6 km	4.1 km
D	9.2 km	6.6 km	4.5 km

#### 4. Conclusions

The approach relies on strict simplifying assumptions on dispersion behaviour according to criteria of representativeness, simplicity, reliability and caution, taking into account, in particular, that carbon dioxide accumulation phenomena on the flat soil are excluded, so that the concentration in the release is overvalued. Upon proper refinement and validation, also in connection with a sound definition of the critical dose based on updated results the framework allows obtaining a single type of general correlation for nearly instantaneous massive release. Upon further validation with field data and simulation runs with reliable tools and refinement, it may help in a preliminary definition of the critical distance of release from an existing industrial activity or natural event, limiting the excessive conservatism of free models such as Aloha.

#### Nomenclature

D – dose, s	u – wind speed, m·s <sup>-1</sup>
h - height of the cloud, m	v <sub>r</sub> – radius grow velocity, m·s <sup>-1</sup>
M <sub>a</sub> – air molecular mass, -	V – cloud volume, m <sup>3</sup>
M <sub>r</sub> – release molecular mass, -	w – mass fraction of CO <sub>2</sub> in the release, -
m <sub>r</sub> – release mass, kg	w <sub>0</sub> – initial mass fraction of CO <sub>2</sub> in the release, -
r – radius of the cloud, m	y – CO <sub>2</sub> concentration, -
r <sub>0</sub> – initial radius of the cloud, m	y <sub>0</sub> – initial CO <sub>2</sub> concentration, -
r <sub>c</sub> –critical distance, m	y <sub>a</sub> –CO <sub>2</sub> concentration in the axis of the cloud, -
r <sub>L</sub> – limit distance of cloud spreading, m·s <sup>-1</sup>	ρ <sub>0</sub> – release density, kg·m <sup>-3</sup>

#### References

- Hansson, A., Bryngelsson, M., 2009. Expert opinions on carbon dioxide capture and storage—a framing of uncertainties and possibilities, *Energy Policy*, 37(6), 2273-2282.
- Le Guéan, T., Manceau, J. C., Bouc, O., Rohmer, J., Ledoux, A. 2011. GERICO: A database for CO<sub>2</sub> geological storage risk management. *Energy Procedia*, 4, 4124-4131.
- Li K., Zhou X., Tu R., Xie Q., Jiang X., 2014. The flow and heat transfer characteristics of supercritical CO<sub>2</sub> leakage from a pipeline. *Energy* 71, 665-672.
- Mazzoldi A., Picard D., Sriram P.G., Oldenburg C.M., 2013. Simulation-based estimates of safety distances for pipeline transportation of carbon dioxide. *Greenhouses Gases: Science and Technology* 3(1), 66–83.
- Palazzi E., Currò F., Lunghi E., Fabiano B., 2016a, An analytical model of carbon dioxide jet from pressurized systems for safety distance evaluation, *Chemical Engineering Transactions* 53, 301-306.
- Palazzi E., Lunghi E., Reverberi A., Fabiano B., 2016b, Large Scale Carbon Dioxide Release: Short-Cut Analytical Modelling and Application, *Chemical Engineering Transactions* 53, 355-360.
- Vairo, T., Pontiggia, M., Fabiano, B. 2021, Critical aspects of natural gas pipelines risk assessments. A case-study application on buried layout, *Process Saf. Environ. Prot.*, 149, 258–268.
- Van Ulden A.P., 1974, On the spreading of a heavy gas released near the ground, 1st Int. Loss. Prev. Symp., Hague/Delft, The Netherlands, 221-226.
- Viebahn, P., Vallentin, D., & Höller, S. 2015. Prospects of carbon capture and storage (CCS) in China's power sector—an integrated assessment, *Applied Energy*, 157, 229-244.
- Webber D.M., 2011, Generalising two-phase homogeneous equilibrium pipeline and jet models to the case of carbon dioxide, *Journal of Loss Prevention in the Process Industries* 24, 356-360.